

# Seismic Reliability Assessment of Classical Columns Subjected to Near Source Ground Motions

Ioannis Stefanou, Michalis Fragiadakis and Ioannis N. Psycharis

**Abstract** Classical columns are articulated structures made of several discrete bulgy stone blocks (drums) put one on top of the other without mortar. Thanks to their unique structural system, many of these structures have survived several strong earthquakes over the centuries. However, many others have collapsed. The dynamic behaviour of these systems is rich, complex and very sensitive to the ground input motion. A performance-based seismic risk assessment methodology for the vulnerability assessment of multidrum columns is discussed and presented on two columns of different size. The first column was inspired by the Parthenon Pronaos and the second from the Propylaia of the Acropolis hill in Athens. The Discrete Element Method (DEM) is adopted in order to simulate the three-dimensional dynamic response of the columns. Limit-state exceedance probabilities are obtained using the Monte Carlo simulation and a series of synthetic ground motion records of varying magnitude and source distance. The results pinpoint the different vulnerability of the two columns and verify that larger columns are more stable compared to smaller with dimensions of the same aspect ratio. The methodology presented may serve as a valuable decision-making tool for the restoration of classical monuments.

**Keywords** Classical monuments · Multidrum masonry columns · Risk assessment · Fragility analysis · 3D distinct element method (DEM) · Performance-based design

---

I. Stefanou (✉)

Université Paris-Est, Laboratoire Navier (ENPC-IFSTTAR-CNRS),  
Ecole Des Ponts Paris Tech, Marne-La-Vallée, France  
e-mail: ioannis.stefanou@enpc.fr

M. Fragiadakis · I.N. Psycharis

Laboratory for Earthquake Engineering, School of Civil Engineering,  
National Technical University of Athens (NTUA), Athens, Greece  
e-mail: mfrag@mail.ntua.gr

I.N. Psycharis

e-mail: ipsych@central.ntua.gr

© Springer International Publishing Switzerland 2015

I.N. Psycharis et al. (eds.), *Seismic Assessment, Behavior and Retrofit of Heritage Buildings and Monuments*, Computational Methods in Applied Sciences 37, DOI 10.1007/978-3-319-16130-3\_3

## 1 Introduction

Classical monuments are commonly made of discrete bulgy stone blocks. A common structural element of these ancient structures is the multidrum column (Fig. 1), which consists of discrete drums stacked one on top of the other without mortar or any other connecting mechanism. During earthquakes, the columns respond with intense rocking, wobbling and, depending on the incipient ground motion, sliding of the drums. In few cases, steel connections (dowels) that restrict sliding are provided at the joints, which, however, do not in general affect rocking.

Several investigators have examined the seismic response of classical monuments and, in general, of stacks of rigid blocks using analytical, numerical and experimental methods. These analyses are mostly two dimensional (e.g. [1–4], among others). Three dimensional analyses are fewer [5–8] but necessary in order to obtain a more faithful representation of the dynamics of these systems. The aforementioned studies have shown that the response is strongly non-linear and quite sensitive even to small changes in the geometry, the mechanical properties or the ground excitation. This is a profound characteristic of these systems and is observed even in the simplest case of a single rigid block under rocking [9]. Previous analyses of the seismic response of classical columns have shown that

**Fig. 1** A column at Propylaia of Acropolis hill in Athens, Greece. Drum dislocation is observed above the bottom drum



these structures, despite their apparent instability to static horizontal loads, are generally earthquake-resistant [10]. This was also proven from the fact that many classical monuments built in seismic prone areas have survived for almost 2500 years. However, many others have collapsed.

The assessment of the seismic reliability/vulnerability of a monument is a prerequisite for rational decision-making during restorations. The seismic vulnerability of the column is vital information that can help the authorities decide the necessary interventions and establish their policy, not only in what concerns the collapse risk, but also the magnitude of the expected maximum and residual displacements of the drums. This assessment is not straightforward, not only because fully detailed analyses are practically impossible due to the sensitivity of the response to small changes in the geometry, but also because the results depend highly on the ground motion characteristics.

This chapter is focused on the evaluation of the seismic risk assessment of multidrum columns such as those of Fig. 1. Two different column geometries are considered and their dynamic behaviour is juxtaposed for a large spectrum of seismic ground motions. To this extent, a specifically tailored performance-based framework for classical monuments is discussed [11]. The probability of exceedance of a number of preset limit states is calculated and presented in the form of fragility surfaces.

In order to account for the random nature of seismic ground motions and the strong non-linearities of the system at hand, the Monte Carlo method was applied using near-source synthetic ground motions records. The response of the columns was calculated and compared for 35  $M_w$ - $R$  scenarios, resulting to 3500 three-dimensional simulations for every column geometry. All simulations were performed using the Discrete Element Method (DEM) and in particular the software 3DEC developed by Itasca (Itasca Consulting Group [12]).

The structure of this Chapter is as follows: Sect. 2 presents the structural model used for the seismic assessment of the columns. Section 3 describes the probabilistic approach followed and Sect. 4 the performance levels that were chosen. Finally, in Sect. 5 the results of the analyses of two typical columns, i.e. of the Propylaia and of the Parthenon Pronaos, are presented and the seismic performance of the columns is compared.

## 2 Numerical Modelling and Properties of the Multidrum Columns Considered

During a seismic event, the response of a multidrum column is dominated by the “spinal” form of the construction and is governed by the sliding, the rocking and the wobbling of the individual, practically rigid, stone drums. The drums may translate and rotate independently or in groups (Fig. 2). There are many ‘modes’ in which the system can vibrate, with different joints being opened depending on the mode

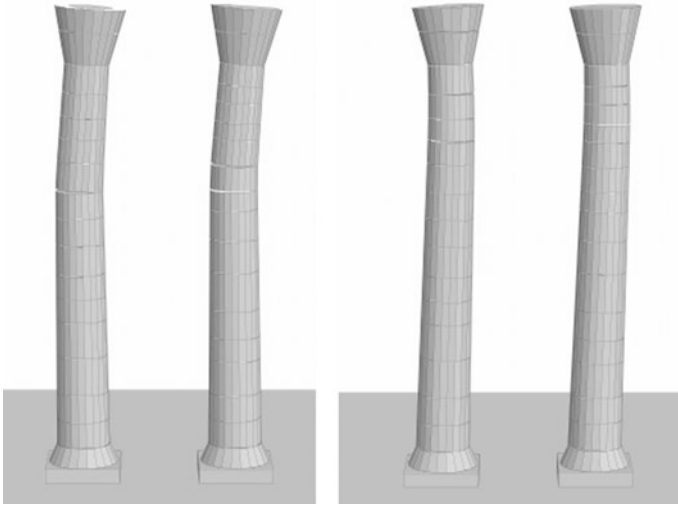


**Fig. 2** Response of two columns of Olympieion of Athens at two different time instances during intense ground shaking. The geometry of the two columns is slightly different (the *left* has 14 drums and the *right* 15) leading to different ‘modes’ of vibration (numerical results obtained with 3DEC software)

examined. Under a strong earthquake excitation the column continuously moves from one oscillation ‘mode’ to another. It is noted that the term ‘mode’ is used here to denote different patterns of the response and does not literally refer to the eigenmodes of the system, since spinal structures do not possess natural modes in the classical sense of structural dynamics.

The underlying mathematical problem is strongly non-linear and consequently the modelling of the dynamic behaviour of multidrum columns is quite complex. Even in the case of systems with a single-degree-of-freedom in the two dimensional space, i.e. a monolithic rocking block, the analytical and the numerical analysis is not trivial [9] and differs from the approaches followed in modern structural analysis. The dynamic response becomes even more complex in three dimensions [8], where realistic models have to account also for non-linearities related to the three-dimensional motion of each drum and the energy dissipation at the joints [7].

The Discrete (or Distinct) Element Method (DEM) is used for the numerical modelling of the seismic response of multidrum systems. Although DEM is not the only choice for the discrete system at hand, it forms an efficient and validated approach for studying the dynamic behaviour of masonry columns in classical monuments. In the analyses presented herein, the Molecular Dynamics (smooth-contact) approach was followed [13] through the use of the three-dimensional DEM code 3DEC [12]. The software used provides the means to apply the conceptual model of a masonry structure as a system of blocks which may be either rigid or deformable. In the present study only rigid blocks were used, as this was found to be a sufficient approximation capable to substantially reduce the

computing time. The system deformation is concentrated at the joints (soft-contacts), where frictional sliding and/or complete separation may take place (dislocations and/or disclinations between blocks). As discussed in more detail by Papantonopoulos et al. [14], the discrete element method employs an explicit algorithm for the solution of the equations of motion, taking into account large displacements and rotations. The efficiency of the method and particularly of 3DEC to capture the seismic response of classical structures has been previously validated with experimental data [5, 14].

The geometry of the columns considered was inspired by the columns of the Propylaia and the Parthenon Pronaos on the Acropolis Hill in Athens (Fig. 3). The Propylaia column is made of seven drums of diameter equal to 1.00 m and height equal to 0.85 m. The total height of the column is approximately 5.95 m. The column of the Parthenon Pronaos is larger and its geometry is more elaborate, as it is part of the Parthenon. It has a total height of 10.08 m, being composed of a shaft of height 9.38 m and a capital. The real column has 20 flutes; however, the shaft in the numerical model was represented in an approximate manner by a pyramidal segment made of blocks of polygonal ten-sided cross section with diameters ranging from 1.65 m at the base to 1.28 m at the top. The shaft was divided into 12 drums of different height according to actual measurements of the columns of the Pronaos (Fig. 3).

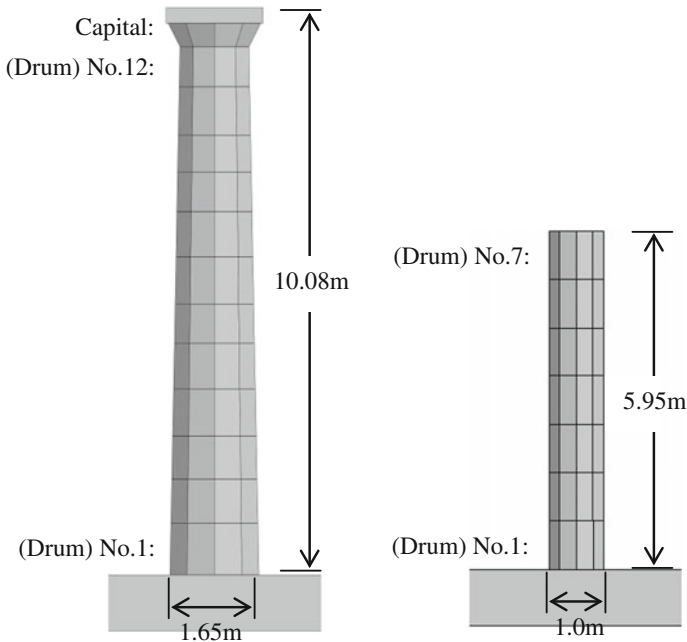


**Fig. 3** The multidrum columns considered in the analyses. On the *left*, the model of the Parthenon Pronaos column and on the *right* the model of the Propylaia column. The Parthenon column is larger and has a more elaborate geometry than the Propylaia column

It is worth mentioning that the two columns have similar slenderness (i.e. height to base diameter ratio) equal to 6.1 in case of the Parthenon–Pronaos and 5.95 in case of Propylaia. Nevertheless, as it will be shown in Sect. 3, the Parthenon Pronaos column, which is bulgier, is more stable than the Propylaia column. This was expected due to the inherent scale effect of such systems [9, 10].

A quite important factor for the numerical analysis is the selection of appropriate constitutive laws that govern the mechanical behaviour of the joints. A Coulomb-type failure criterion was chosen in the present study. Table 1 lists the friction angle, the cohesion, the ultimate tensile strength (zero) and the stiffness of the joints. It is noted that the stiffness might affect considerably the results of the analysis. A parametric investigation performed by Toumbakari and Psycharis [15] showed that stiff joints might lead to larger permanent dislocations of all drums for strong ground motions compared with joints of soft stiffness. The values presented in Table 1 correspond to marble columns and were calibrated against shaking table experiments of free-standing columns [14]; with these values, good agreement was achieved concerning both the maximum top displacement and the residual displacements of the drums. It must be pointed out, however, that different values should be assigned to the stiffness parameters for material other than marble of good quality.

No artificial (numerical) damping was introduced to the system. According to the results of a previous investigation [14], damping can be set to zero only during intense rocking response, while non-zero damping should be considered after that period in order to dissipate the free vibrations and make possible the estimation of permanent deformations. According to reference [15], the value of damping that is used at the end of the strong motion and the time instant that it is introduced, do not affect significantly the response and the estimation of the residual displacements. Therefore, damping was set to zero for the whole time history and only frictional dissipation was considered. This assumption also reduces the runtime of analysis, as damping generally decreases the time step. Since the free rocking oscillations after the end of the strong ground motion were not dissipated, the residual deformation of the column was calculated from the average displacements of the drums during the last 2 s of the response. For more details the reader should consult Psycharis et al. [11].

No connections were considered between the drums, as the only connectors present in the original structure are wooden dowels, the so-called ‘empolia’. It is believed that empolia were used in antiquity in order to centre the drums during their erection and not as a mechanism that provides shear resistance. The shear strength of the wooden dowels is small and hence it is believed that they have a rather marginal effect on the seismic response of the column (cf. [2]).

**Table 1** Constitutive parameters for the Coulomb elastoplastic model considered for the mechanical behaviour of the joints

Normal stiffness	1 GPa/m
Shear stiffness	1 GPa/m
Friction angle	37°
Cohesion	0 MPa
Tensile strength	0 MPa

### 3 Fragility Assessment

Fragility (or vulnerability) curves are a valuable tool for the seismic risk assessment of a system. Fragility analysis was initially developed for the reliability analysis of nuclear plants in an effort to separate the structural analysis part from the hazard analysis performed by engineering seismologists. Vulnerability analysis requires the calculation of the probabilities that a number of monotonically increasing limit-states are exceeded. Therefore, the seismic fragility  $F_R$  is defined as the limit-state probability conditioned on seismic intensity. The seismic intensity can be expressed in terms of magnitude  $M_w$  and distance  $R$ , resulting to a surface  $F_R(M_w, R)$ . Therefore, the fragility of a system is the probability that an engineering demand parameter ( $EDP$ ) exceeds a threshold value  $edp$  and is defined as:

$$F_R(M_w, R) = P(EDP \geq edp | M_w, R) \quad (1)$$

Equation (1) provides a single point of a limit-state fragility surface, while engineering demand parameters ( $EDPs$ ) are quantities that characterise the system response, e.g., maximum deformation or permanent drum dislocation. To calculate  $F_R$ , Monte Carlo Simulations (MCS) with Latin Hypercube Sampling (LHS) were performed for a range of magnitude and distance ( $M_w, R$ ) scenarios. For this purpose, a large number of nonlinear response history analyses for every  $M_w$ - $R$  pair is needed, especially when small probabilities are sought. Therefore, suites of records that correspond to the same  $M_w$  and  $R$  value must be compiled. Since it is very difficult to come up with such suites of natural ground motion records, synthetic ground motions of given  $M_w$  and  $R$  were produced [11].

Assuming that the seismic data are lognormally distributed,  $F_R(M_w, R)$  can be calculated analytically once the mean and the standard deviation of the logs of the  $EDP$  are calculated, which are denoted as  $\mu_{\ln EDP}$  and  $\beta_{\ln EDP}$ , respectively. Once they are known they can be used to calculate  $F_R$  using the standard normal distribution formula:

$$F_R = P(EDP \geq edp | M_w, R) = 1 - \Phi\left(\frac{\ln(edp) - \mu_{\ln EDP}}{\beta_{\ln EDP}}\right) \quad (2)$$

where  $edp$  is the  $EDP$ 's threshold value that denotes that the limit-state examined is violated and  $\Phi$  denotes the standard normal distribution. For example, if one calculates the fragility surface that corresponds to the normalised displacement of the column's capital  $u_{top}$  (defined in the ensuing) larger than 0.3, then  $\ln(edp)$  would be equal to  $\ln(0.3)$ . Alternatively, a good approximation of Eq. (1) can be obtained by the ratio of successful simulations over the total number of simulations performed, thus bypassing the assumption of lognormality. For the case studies examined in this chapter, the two approaches gave close results.

As the ground motion intensity increases, some records may collapse the structure. When collapsed simulations exist, Eq. (2) is not accurate, since the  $EDP$

takes an infinite or a very large value that cannot be used to calculate  $\mu_{\ln EDP}$  and  $\beta_{\ln EDP}$ . To handle such cases, Eq. (2) is modified by separating the data to collapsed and non-collapsed. The conditional probability of collapse is then calculated as:

$$P(C|M_w, R) = \frac{\text{number of simulations collapsed}}{\text{total number of simulations}} \quad (3)$$

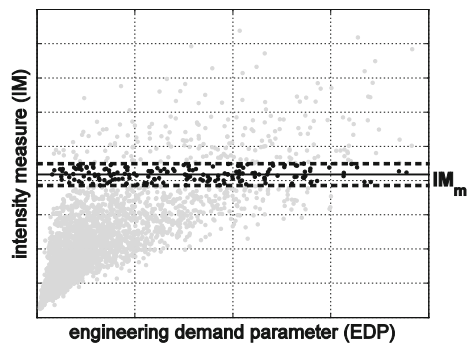
If  $\mu_{\ln EDP}$  and  $\beta_{\ln EDP}$  are the mean and the standard deviation of the non-collapsed data respectively, Eq. (2) is now written:

$$P(EDP \geq edp | M_w, R) = P(C | M_w, R) + (1 - P(C | M_w, R)) \cdot \left( 1 - \Phi \left( \frac{\ln(edp) - \mu_{\ln EDP}}{\beta_{\ln EDP}} \right) \right) \quad (4)$$

Moreover, it is customary to produce fragility curves using a single scalar intensity measure  $IM$ . Thus, instead of conditioning  $F_R$  on magnitude and distance (Eq. (1)) one can use a scalar intensity measure  $IM$  resulting to a fragility curve  $F_R$  ( $IM$ ). Typical intensity measures are the peak ground acceleration ( $PGA$ ), the peak ground velocity ( $PGV$ ), the spectral acceleration ( $SA$ ), the spectral velocity ( $SV$ ), or any other variable that is consistent with the specification of seismic hazard. This option is often preferred, not only because 2D plots are easier to interpret than three-dimensional surfaces but, mainly, because this option is easier in terms of handling the ground motion records. Usually the ground motions are scaled at the same  $IM$  value in order to calculate conditional probabilities. Record scaling is a thorny issue that may introduce biased response estimates and therefore this option was not preferred.

Fragility curves can be alternatively produced through smart post-processing the data. If the data are plotted in  $EDP-IM$  ordinates, the conditional probabilities can be calculated by dividing the  $IM$  axis into stripes, regardless of their  $M_w$  and  $R$  value, as shown in Fig. 4. If  $IM_m$  is the  $IM$  value of the stripe, the conditional probability  $P(EDP \geq edp | IM_m)$  is calculated according to Eq. (2) or (4) using only the data banded within the stripe. Thus, according to Fig. 4, if the moving average  $\mu_{\ln EDP}$  and the dispersion  $\beta_{\ln EDP}$  are calculated using only the black dots,

**Fig. 4** Post-processing to obtain fragility curves from scattered data





$P(EDP \geq edp | IM_m)$  can be approximately calculated using Eq. (4). Some readers may assume that the coupling between  $M_w-R$  and an  $IM$  can be easily obtained using a ground motion prediction equation (also known as attenuation relationship). However, this should be avoided, since ground motion prediction equations have significant scatter and should not be used in this manner.

Synthetic accelerograms that combine a high and a low frequency pulse were used. Synthetic records are more preferable than natural ground motions, due to the limited number of the latter for the range of pairs  $M_w-R$  examined, especially for stiff soil conditions on which such monuments are typically founded. The synthetic records were generated using the process proposed by Mavroeidis and Papageorgiou [16], which allows for the combination of independent models that describe the low-frequency (long period) component of the directivity pulse, with models that describe the high-frequency component of an acceleration time history. A successful application of this approach is given in Taflanidis et al. [17]. In the present research, the generation of the high-frequency component was based on the stochastic approach assuming a point source, as proposed in Boore [18]. Based on a given magnitude-distance scenario ( $M_w-R$ ) and depending on a number of site characteristics, the stochastic approach produces synthetic ground motions. It is noted that the use of point-source models is not appropriate for near-fault ground motions; however, this approach is adopted here for simplicity and is not expected to significantly affect our risk assessment calculations. More details regarding the generation of the synthetic ground motions are given in Psycharis et al. [11].

It must be noted that, due to the high nonlinear nature of the rocking/wobbling response and the existence of a minimum value of the peak ground acceleration that is required for the initiation of rocking, the high frequency part of the records is necessary for the correct simulation of surrogate ground motions. Long-period directivity pulses alone, although they generally produce devastating effects to classical monuments, might not be capable to produce intense shaking and collapse, as their peak acceleration is usually small and not strong enough to even initiate rocking.

Classical monuments were usually constructed on the Acropolis of ancient cities, i.e. on top of cliffs; thus, most of them are founded on stiff soil or rock, and only few of them are built on soft soil. For this reason, the effect of the soil on the characteristics of the exciting ground motion was not considered. It is noted, however, that, although the directivity pulse contained in near-fault records is not generally affected by the soil conditions, soft soil can significantly alter the frequency content of the ground motion and, consequently, affect the response of classical columns. This effect, however, is beyond the scope of this chapter.

## 4 Seismic Performance-Based Assessment

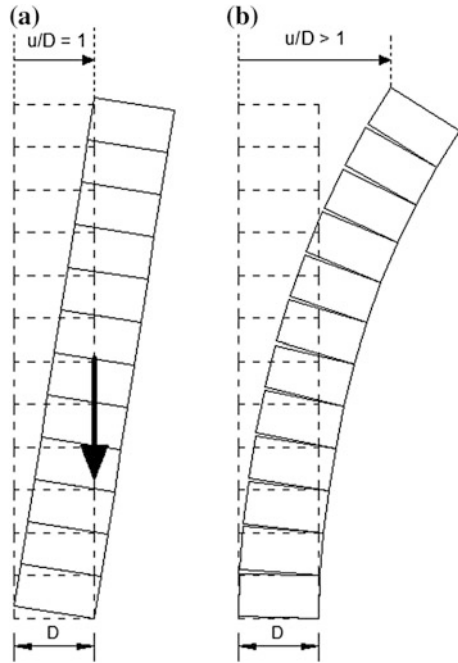
In order to assess the risk of a system, the performance levels of interest and the corresponding levels of capacity of the monument need first to be decided. Demand and capacity should be measured with appropriate parameters (e.g. stresses, strains,

displacements) at critical locations and in accordance to the principal damage (or failure) modes of the structure. Subsequently, this information has to be translated into one, or a combination, of engineering demand parameters (*EDPs*), e.g., maximum column deformation, permanent drum dislocations, foundation rotation or maximum axial and shear stresses. For the *EDPs* chosen, appropriate threshold values that define the various performance objectives e.g. light damage, collapse prevention, etc. need to be established. Since such threshold values are not always directly related to visible damage, the *EDPs* should be related to damage that is expressed in simpler terms, e.g., crack width, crack density or exfoliation surface area. In all, this is a challenging, multi-disciplinary task that requires experimental verification, expert opinion and rigorous formulation.

Two engineering demand parameters (*EDPs*) are introduced for the vulnerability assessment of classical columns: (a) the maximum displacement at the capital normalised by the base diameter (lower diameter of drum No. 1, see Fig. 3); and (b) the relative residual dislocation of adjacent drums normalised by the diameter of the corresponding drums at their interface. The first *EDP* is the maximum of the normalised displacement of the capital (top displacement) over the whole time history and is denoted as  $u_{\text{top}}$ , i.e.  $u_{\text{top}} = \max[u(\text{top})]/D_{\text{base}}$ . This is a parameter that provides a measure of how much a column has been deformed during the ground shaking and also shows how close to collapse the column was brought during the earthquake. Note that the top displacement usually corresponds to the maximum displacement of all drums. The second *EDP* is the residual relative drum dislocations at the end of the seismic motion. This parameter is normalised by the drum diameter at the corresponding joints and is denoted as  $u_{\text{d}}$ , i.e.  $u_{\text{d}} = \max(\text{res}u_i)/D_i$ .  $u_{\text{d}}$  provides a measure of how much the geometry of the column has been altered after the earthquake and thus measures the vulnerability of the column to future events.

The proposed *EDP*'s have a clear physical meaning and allow to easily identify various damage states and to set empirical performance objectives. For example a  $u_{\text{top}}$  value equal to 0.3 indicates that the maximum displacement was 1/3 of the bottom drum diameter and thus there was no danger of collapse. Values of  $u_{\text{top}}$  larger than one imply intense shaking and large deformations of the column, which, however, do not necessarily lead to collapse. It is not easy to assign a specific value of  $u_{\text{top}}$  that corresponds to collapse, as collapse depends on the 'mode' of deformation, which in turn depends on the ground motion characteristics. For example, for a cylindrical column that responds as a monolithic block with a pivot point at the corner of its base (Fig. 5a), collapse is probable to occur for  $u_{\text{top}} > 1$ , as the weight of the column switches from a restoring ( $u_{\text{top}} < 1$ ) to an overturning force. But, if the same column responds as a multidrum spinal system with rocking at all joints (Fig. 5b), a larger value of  $u_{\text{top}}$  can be attained without threatening the overall stability of the column. In fact, the top displacement can be larger than the base diameter without collapse, as long as the weight of each part of the column above an opening joint gives a restoring moment about the pole of rotation of the specific part. In the numerical analyses presented here, the maximum value of  $u_{\text{top}}$  that was attained without collapse was in the order of 1.15.

**Fig. 5** Top displacement for two extreme modes of rocking: **a** as a monolithic block; **b** with opening of all joints (displacements are shown exaggerated)



For the normalised displacement of the capital ( $u_{top}$ ), three performance levels were selected (Table 2), similarly to those that are typically assigned to modern structures. The first level (*damage limitation*) corresponds to weak shaking of the column with very small or no rocking. At this level of shaking, no damage, nor any severe residual deformations, is expected. The second level (*significant damage*) corresponds to intense shaking with significant rocking and evident residual deformation of the column after the earthquake; however, the column is not brought close to collapse. The third performance level (*near collapse*) corresponds to very intense shaking with significant rocking and probably sliding of the drums. The column does not collapse at this level, as  $u_{top} < 1$ , but it is brought close to collapse. In most cases, collapse occurred when this performance level was exceeded. The values of  $u_{top}$  that are assigned at every performance level are based on the average assumed risk of collapse.

**Table 2** Proposed performance criteria based on the normalized displacement of the capital  $u_{top}$

$u_{top}$	Performance level	Description
0.15	Damage limitation	No danger for the column. No permanent drum dislocations expected
0.35	Significant damage	Large opening of the joints with probable damage due to impacts and considerable residual dislocation of the drums. No serious danger of collapse
1.00	Near collapse	Very large opening of the joints, close to partial or total collapse

**Table 3** Proposed performance based on the normalized residual drum dislocations,  $u_d$ 

$u_d$	Performance level	Description
0.005	Limited deformation	Insignificant residual drum dislocations without serious effect to future earthquakes
0.01	Light deformation	Small drum dislocations with probable unfavourable effect to future earthquakes
0.015	Significant deformation	Large residual drum dislocations that increase significantly the danger of collapse during future earthquakes

Three performance levels were also assigned to the normalised residual drum dislocation,  $u_d$  (Table 3). This *EDP* is not directly related to how close to collapse the column was brought during the earthquake, since residual displacements are caused by wobbling and sliding and are not, practically, affected by the amplitude of the rocking. However, their importance to the response of the column to future earthquakes is significant, as previous damage/dislocation has generally an unfavourable effect to the seismic capacity of the system [19].

The first performance level (*limited deformation*) concerns very small residual deformation, which is not expected to affect considerably the response of the column to future earthquakes. The second level (*light deformation*) corresponds to considerable drum dislocations that might affect the dynamic behaviour of the column to forthcoming earthquakes, increasing its vulnerability. The third performance level (*significant deformation*) refers to large permanent displacements at the joints that increase considerably the danger of collapse to future strong seismic motions. It must be noted that the threshold values assigned to  $u_d$  are not obvious, as the effect of pre-existing damage to the dynamic response of the column varies significantly according to the column properties and the characteristics of the ground motion. The threshold values here proposed are based on engineering judgment taking into consideration the size of drum dislocations that have been observed in monuments and also the experience of the authors from previous numerical analyses and experimental tests. It is noted that, according to the results of this study, the first limit case was exceeded by most of the records examined, while the third case was exceeded only by a few ground motions.

## 5 Fragility Assessment of the Propylaia and the Parthenon Pronaos Columns

The proposed fragility assessment methodology was applied to a typical multidrum column of the Propylaia and to a typical column of Parthenon Pronaos (Fig. 3). The response of each column was calculated for 35  $M_w$ - $R$  scenarios. For every  $M_w$ - $R$  scenario 100 Monte Carlo Simulations (MCS) were performed resulting to 3500 simulations per each column considered. The columns have almost the same slenderness but their size is different (Fig. 3).

### 5.1 Propylaia Multidrum Column

Figure 6 presents the collapse probabilities of the Propylaia column as function of the earthquake magnitude and the distance from the fault. Collapse is considered independently of whether it is local (collapse of a few top drums) or total (collapse of the whole column). Apparently, the number of collapses is larger for smaller fault distances and larger magnitudes. For instance, for  $M_w = 7.5$  and  $R = 5$  km, 70 % of the simulations resulted to collapse. However, practically zero collapses occurred for magnitudes less than 6.0.

Concerning the mean top displacement during the seismic motion, Fig. 7 shows that for small distances from the fault, up to approximately 7.5 km, the mean value of  $u_{top}$  increases monotonically with the magnitude. However, for larger fault distances, the maximum  $u_{top}$  occurs for magnitude  $M_w = 6.5$  whilst for larger  $M_w$  the top displacement decreases. This counter-intuitive response is attributed to the saturation of the  $PGV$  for earthquakes with magnitude larger than  $M_{sat} = 7.0$ , while,

**Fig. 6** Collapse probabilities of the Propylaia multidrum column

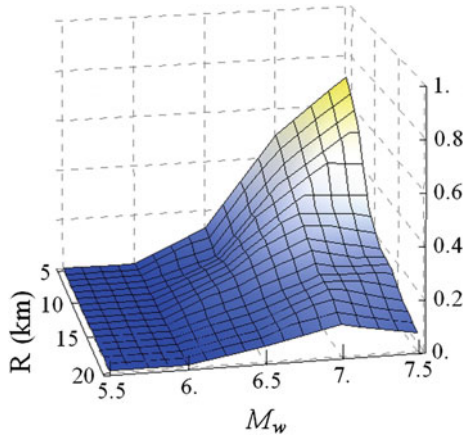
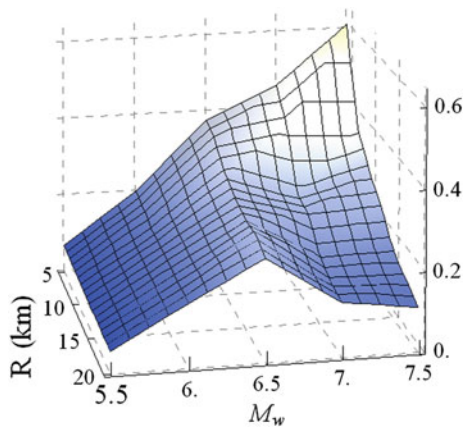


**Fig. 7** Mean maximum normalised top displacements,  $u_{top}$ , for the Propylaia multidrum column



according to commonly used ground motion prediction equations, the period of the pulse increases exponentially with the magnitude. As a result, the directivity pulse has small acceleration amplitude for large magnitudes, which is not capable to produce intense rocking. This ‘strange’ behaviour was also verified using natural ground motion records [11].

Figure 8 presents the fragility surfaces of the Propylaia column for the three performance levels, where  $u_{\text{top}}$  ranges from *significant damage* ( $u_{\text{top}} > 1$ ) to *damage limitation* ( $u_{\text{top}} > 0.15$ ). It is reminded that  $u_{\text{top}} > 0.15$  means that the maximum top displacement during the ground shaking is larger than 15 % of the base diameter and  $u_{\text{top}} > 1$  corresponds to intense rocking, close to collapse. When *damage limitation* is examined (Fig. 8c), the exceedance probability is 0.6 for  $M_w = 6$  and increases for ground shakings of larger magnitude. For the worst scenario among those examined ( $M_w = 7.5$ ,  $R = 5$  km), the probability that the top displacement is larger than 15 % of  $D_{\text{base}}$  during ground shaking, is equal to one, while in the range  $M_w = 6.5\text{--}7.5$  and  $R > 15$  km a decrease in the exceedance probability is observed (likelihood).

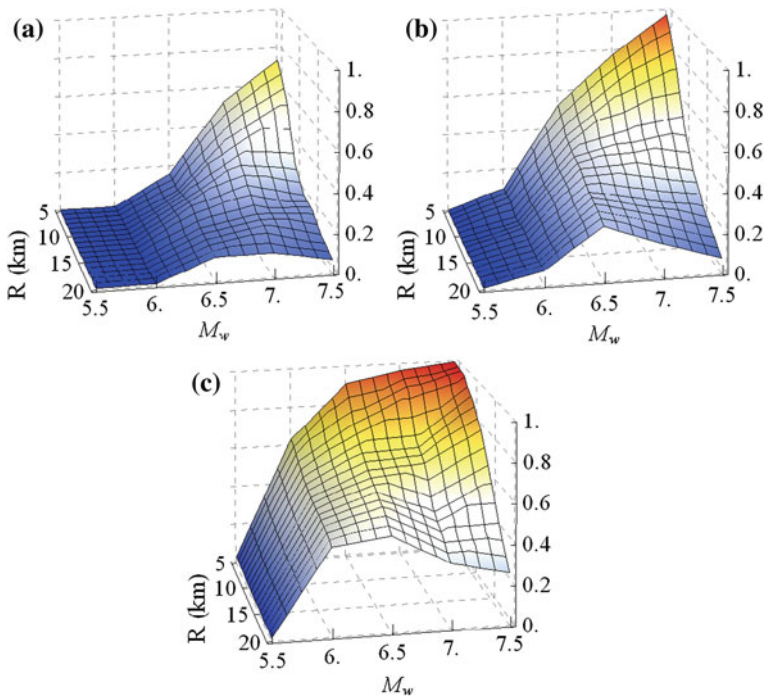


**Fig. 8** Fragility surfaces related to column collapse for the Propylaia column for the performance levels of Table 2: **a**  $P(u_{\text{top}} > 1.0)$ ; **b**  $P(u_{\text{top}} > 0.35)$ ; **c**  $P(u_{\text{top}} > 0.15)$

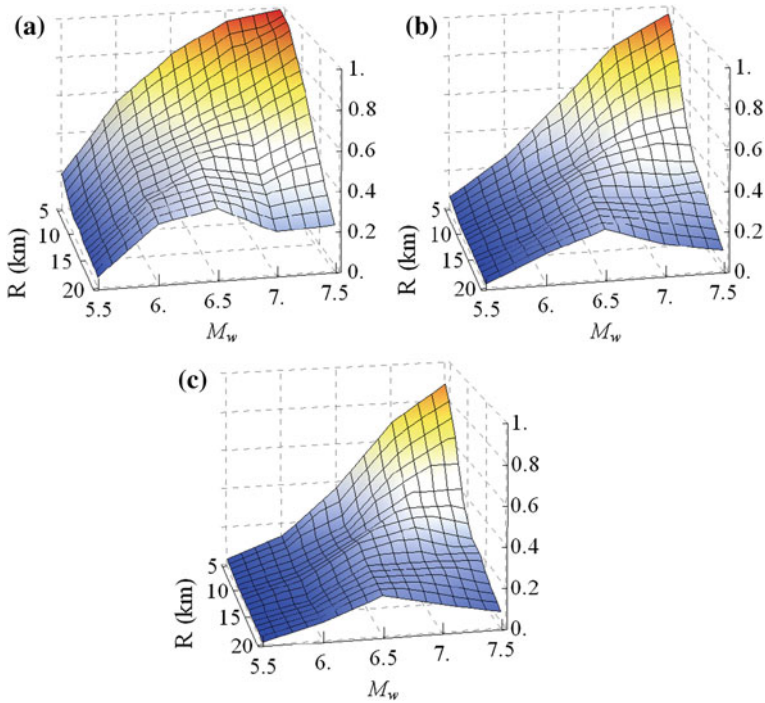


**Fig. 9** Fragility surfaces with respect to the permanent drum dislocations for the Propylaia column and for the performance levels of Table 3: **a**  $P(u_d > 0.005)$ ; **b**  $P(u_d > 0.01)$ ; **c**  $P(u_d > 0.015)$

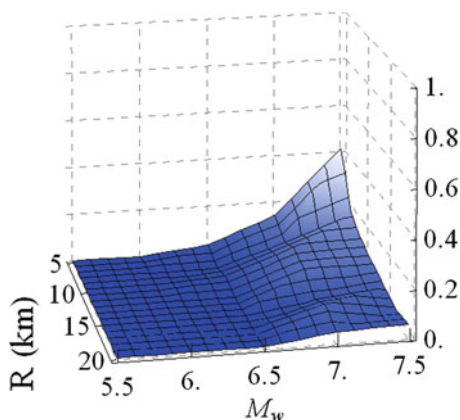
Similar observations hold for the exceedance of the *significant damage* limit state ( $u_{top} > 0.35$ ), but the probability values are smaller. For the *near collapse* limit state ( $u_{top} > 1.0$ ), the probability of exceedance is reduced significantly for large distances, even for large magnitudes. Notice that the  $u_{top} > 1.0$  fragility surface is quite similar to the probability of collapse of Fig. 6, which shows that, if the top displacement reaches a value equal to the base diameter, then there is a big possibility that the column will collapse a little later.

Figure 9 shows the fragility surfaces when the *EDP* is the normalised permanent drum dislocation,  $u_d$ . For the *limited deformation* limit state ( $u_d > 0.005$ ), probabilities around 0.5 are observed for magnitudes close to 6 and  $R$  equal to 10 to 15 km. For the Propylaia column whose drum diameter is 1000 mm (Fig. 2),  $u_d > 0.005$  refers to residual displacements at the joints exceeding 5 mm. The probability of exceedance of the *light deformation* performance criterion ( $u_d > 0.01$ ), which corresponds to residual drum dislocations larger than 10 mm, is less than 0.20 while the probability of exceedance of the *significant deformation* limit state ( $u_d > 0.015$ ) was less than 0.10 for fault distances larger than 10 km.

## 5.2 The Parthenon Pronaos Column

The same methodology was applied on the column of the Parthenon Pronaos. The collapse probabilities of the column are shown in Fig. 10. As before, collapse of the column is considered regardless of whether it is local (collapse of a few upper drums) or total (complete collapse of the column). Similarly to the Propylaia column, the number of collapses is larger for smaller fault distances and larger magnitudes (Fig. 10). For  $M_w = 7.5$  and  $R = 5$  km, 40 % of the simulations resulted to collapse, but practically zero collapses occurred for magnitudes less than 6.5. Figure 11 shows the normalised mean top displacement during the seismic motion. As already discussed  $PGV$  saturates for magnitudes above  $M_{w,sat} = 7.0$  and therefore a decrease of the normalised maximum top displacement is observed. Figure 12 shows the fragility surfaces of the Parthenon column for the three performance levels of Table 2. Again we note that the  $u_{top} > 1.0$  fragility surface practically coincides with the collapse probability of Fig. 10. Concerning the normalised permanent drum dislocation,  $u_d$  (Table 3), the probability of exceedance *limited deformation* limit state ( $u_d > 0.005$ ) is around 0.3 for magnitudes close to 6 (Fig. 13). Note that, for the column of the Parthenon Pronaos with an average drum diameter about 1600 mm (Fig. 2),  $u_d > 0.005$  refers to residual displacements at the joints exceeding 8 mm. The probability of exceedance of the *light deformation* performance criterion ( $u_d > 0.01$ ), which corresponds to residual drum dislocations larger than 16 mm, is less than 0.2 for all earthquake magnitudes and for fault distances that exceed 10 km. The *significant deformation* limit state ( $u_d > 0.015$ ) was exceeded only in a few cases (Fig. 13).

**Fig. 10** Collapse probabilities of the Parthenon Pronaos column





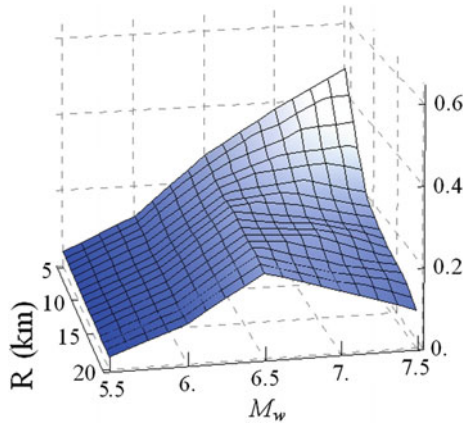


**Fig. 11** Mean maximum normalised top displacements,  $u_{top}$ , for the Parthenon Pronaos multidrum column

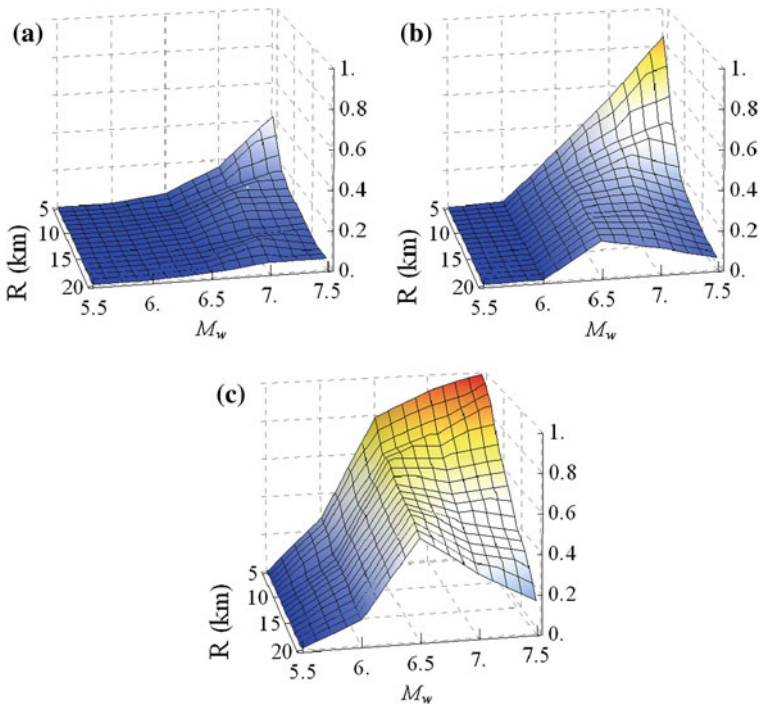


**Fig. 12** Fragility surfaces related to column collapse for the Parthenon Pronaos column for the performance levels of Table 2: **a**  $P(u_{top} > 1.0)$ ; **b**  $P(u_{top} > 0.35)$ ; **c**  $P(u_{top} > 0.15)$

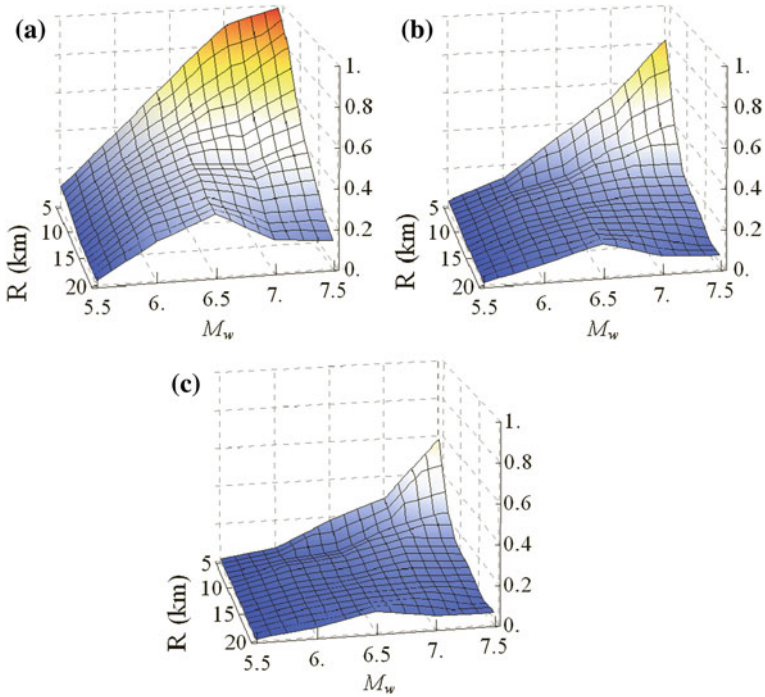


**Fig. 13** Fragility surfaces with respect to the permanent drum dislocations for the Parthenon Pronaos column and for the performance levels of Table 3: **a**  $P(u_d > 0.005)$ ; **b**  $P(u_d > 0.01)$ ; **c**  $P(u_d > 0.015)$

### 5.3 Comparison

Figure 14 compares the vulnerabilities of the two columns with respect to  $u_{top}$ . Clearly the Parthenon Pronaos column is less vulnerable than the column of the Propylaia. This is in accordance with the rule that larger columns are more stable than smaller ones of the same aspect ratio (size/scale effect). This was first discussed by Housner [9] who examined the response of rigid blocks, while Psycharis et al. [10] showed that the scale effect also holds for multidrum classical columns. Another difference between the two columns is the number of the drums (7 for the Propylaia and 13 for the Parthenon column). However, previous parametric

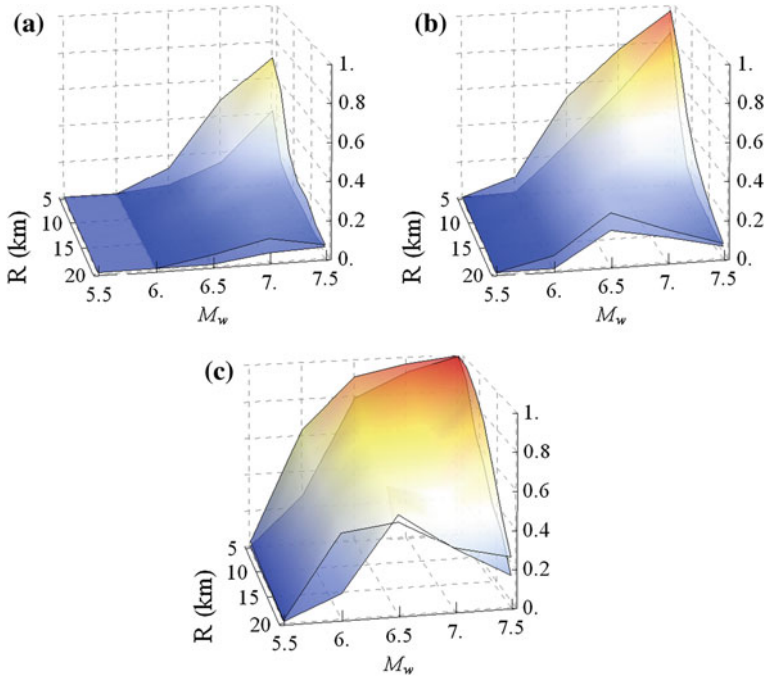


**Fig. 14** Comparison of the fragility surfaces related to column collapse between the Propylaia (*top surfaces*) and the Parthenon Pronaos (*bottom surfaces*) columns for the performance levels of Table 2: **a**  $P(u_{top} > 1.0)$ ; **b**  $P(u_{top} > 0.35)$ ; **c**  $P(u_{top} > 0.15)$ . In all cases, the probabilities of exceedance of each threshold are higher for the smaller column, viz. the Propylaia column

investigations on a column with dimensions same to those of the Propylaia column showed that the number of drums has a rather small impact on the probability of collapse [10, 20].

With respect to the permanent deformations,  $u_d$ , the performance of both columns is comparable (Fig. 15). However, the residual dislocations of the Propylaia column are higher in all cases, while the difference with the Parthenon column is smaller for lower performance levels. Thus, the smaller difference is observed for  $P(u_d > 0.005)$  and the larger for  $P(u_d > 0.015)$ . In the latter case, the probability of exceedance of  $u_d = 0.015$  for small fault distances and large earthquake magnitudes is almost double for the Propylaia column compared with the Parthenon column.

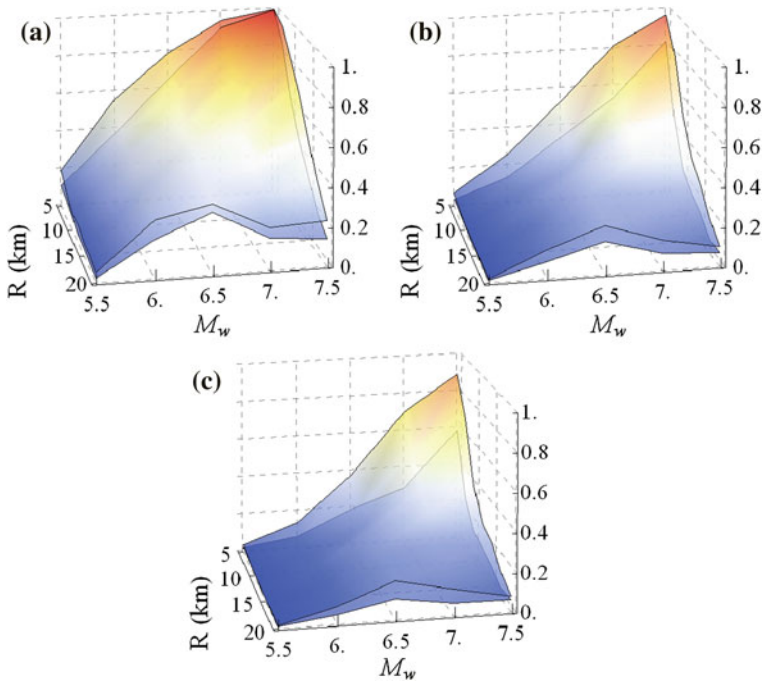


**Fig. 15** Comparison of the fragility surfaces related to the permanent drum dislocations ( $u_d$ ) between the Propylaia (*top surfaces*) and the Parthenon Pronaos (*bottom surfaces*) columns for the performance levels of Table 3: **a**  $P(u_d > 0.005)$ ; **b**  $P(u_d > 0.01)$ ; **c**  $P(u_d > 0.015)$ . In all cases, the probabilities of exceedance of each threshold are higher for the smaller column, viz. the Propylaia column

## 6 Conclusions

The seismic risk assessment of two multidrum columns of similar slenderness but of different size and number of blocks was performed. In order to account for the probabilistic nature of the seismic events and the strong nonlinearities of the dynamical system at hand, the Monte Carlo method was applied using synthetic ground motions which contain a high- and a low-frequency component. The response of the columns was calculated and compared for 35  $M_w$ – $R$  scenarios resulting to 3500 analyses for each column.

An engineering demand parameter (*EDP*) related to the column collapse risk was adopted for the assessment of the vulnerability of the considered multidrum columns. The fragility analysis verified that the vulnerability is higher for the smaller in size column (Propylaia column). For instance, the probability of collapse of the Propylaia column was found almost twice that of the Parthenon Pronaos column. For an earthquake of  $M_w = 7.5$  at distance  $R = 5$  km, the probability of collapse of

the column of the Parthenon Pronaos is 40 %, while the corresponding probability of the Propylaia column is approximately 70 %. This corroborates the fact that larger columns are more stable than smaller of the same aspect ratio. This scale effect was first noticed by Housner [9] for rocking blocks and, later, was also proved for multidrum columns [10] (in two dimensions). It is now extended to multidrum columns in three dimensions, which show a more complex dynamic behaviour, as it is verified statistically for a large sample of earthquakes of different magnitude and distance from the seismic source.

Regarding permanent deformations, the columns of smaller size seem to develop larger residual deformations for strong ground motions. Nevertheless, for moderate earthquakes, the permanent deformations of smaller columns are comparable with the permanent deformations of larger columns.

## References

1. Allen RH, Oppenheim IJ, Parker AR, Bielak J (1986) On the dynamic response of rigid body assemblies. *Earthq Eng Struct Dyn* 14:861–876. doi:[10.1002/eqe.4290140604](https://doi.org/10.1002/eqe.4290140604)
2. Konstantinidis D, Makris N (2005) Seismic response analysis of multidrum classical columns. *Earthq Eng Struct Dyn* 34:1243–1270. doi:[10.1002/eqe.478](https://doi.org/10.1002/eqe.478)
3. Psycharis IN (1990) Dynamic behaviour of rocking two-block assemblies. *Earthq Eng Struct Dyn* 19:555–575. doi:[10.1002/eqe.4290190407](https://doi.org/10.1002/eqe.4290190407)
4. Sinopoli A (1991) Dynamic analysis of a stone column excited by a sine wave ground motion. *Appl Mech Rev* 44:S246. doi:[10.1115/1.3121361](https://doi.org/10.1115/1.3121361)
5. Dasiou M, Psycharis IN, Vayas I (2009) Verification of numerical models used for the analysis of ancient temples. Prohitech Conference, Rome
6. Psycharis IN, Lemos JV, Papastamatiou DY et al (2003) Numerical study of the seismic behaviour of a part of the Parthenon Pronaos. *Earthq Eng Struct Dyn* 32:2063–2084. doi:[10.1002/eqe.315](https://doi.org/10.1002/eqe.315)
7. Stefanou I, Psycharis IN, Georgopoulos I (2011) Dynamic response of reinforced masonry columns in classical monuments. *Constr Build Mater* 25:4325–4337. doi:[10.1016/j.conbuildmat.2010.12.042](https://doi.org/10.1016/j.conbuildmat.2010.12.042)
8. Stefanou I, Vardoulakis I, Mavraganis A (2011) Dynamic motion of a conical frustum over a rough horizontal plane. *Int J Non Linear Mech* 46:114–124. doi:[10.1016/j.ijnonlinmec.2010.07.008](https://doi.org/10.1016/j.ijnonlinmec.2010.07.008)
9. Housner GW (1963) The behavior of inverted pendulum structures during earthquakes. *Bull Seismol Soc Am* 53:403–417
10. Psycharis IN, Papastamatiou DY, Alexandris AP (2000) Parametric investigation of the stability of classical columns under harmonic and earthquake excitations. *Earthq Eng Struct Dyn* 29:1093–1109. doi:[10.1002/1096-9845\(200008\)29:8<1093::AID-EQE953>3.0.CO;2-S](https://doi.org/10.1002/1096-9845(200008)29:8<1093::AID-EQE953>3.0.CO;2-S)
11. Psycharis IN, Fragiadakis M, Stefanou I (2013) Seismic reliability assessment of classical columns subjected to near-fault ground motions. *Earthq Eng Struct Dyn* 42:2061–2079. doi:[10.1002/eqe.2312](https://doi.org/10.1002/eqe.2312)
12. Itasca Consulting Group 3DEC. Three dimensional distinct element code
13. Cundall PA, Strack ODL (1979) A discrete numerical model for granular assemblies. *Géotechnique* 29:47–65. doi:[10.1680/geot.1979.29.1.47](https://doi.org/10.1680/geot.1979.29.1.47)
14. Papantonopoulos C, Psycharis IN, Papastamatiou DY et al (2002) Numerical prediction of the earthquake response of classical columns using the distinct element method. *Earthq Eng Struct Dyn* 1717:1699–1717. doi:[10.1002/eqe.185](https://doi.org/10.1002/eqe.185)

15. Toumbakari E, Psycharis IN (2010) Parametric investigation of the seismic response of a column of the aphrodite temple in amathus, cyprus. In: 14th european conference earthquake engineering, Ohrid, FYROM, 30 Aug–3 Sept
16. Mavroeidis GP, Papageorgiou AS (2003) A mathematical representation of near-fault ground motions. *Bull Seismol Soc Am* 93:1099–1131
17. Taflanidis AA, Scruggs JT, Beck JL (2008) Probabilistically robust nonlinear design of control systems for base-isolated structures. *Struct Control Heal Monit* 697–719. doi: [10.1002/stc](https://doi.org/10.1002/stc)
18. Boore DM (2003) Simulation of ground motion using the stochastic method. *Pure appl Geophys* 160:653–676
19. Psycharis IN (2007) A probe into the seismic history of Athens, Greece from the current state of a classical monument. *Earthq Spectra* 23:393–415. doi:[10.1193/1.2722794](https://doi.org/10.1193/1.2722794)
20. Ntetsika M (2013) The dynamic response of multi-drum columns. Thesis, Ecole Nationale des Ponts et Chaussées